Time Crystal Platform: From Quasicrystal Structures in Time to Systems with Exotic Interactions

Krzysztof Giergiel,[1] Artur Miroszewski,[1,2] and Krzysztof Sacha[1,3]
[1]*Instytut Fizyki imienia Mariana Smoluchowskiego, Uniwersytet Jagielloński, ulica Profesora Stanisława Łojasiewicza 11, PL-30-348 Kraków, Poland*
[2]*National Centre for Nuclear Research, ul.Hoża 69, PL-00-681 Warsaw, Poland*
[3]*Mark Kac Complex Systems Research Center, Uniwersytet Jagielloński, ulica Profesora Stanisława Łojasiewicza 11, PL-30-348 Kraków, Poland*

(Received 21 November 2017; published 2 April 2018)

Time crystals are quantum many-body systems that, due to interactions between particles, are able to spontaneously self-organize their motion in a periodic way in time by analogy with the formation of crystalline structures in space in condensed matter physics. In solid state physics properties of space crystals are often investigated with the help of external potentials that are spatially periodic and reflect various crystalline structures. A similar approach can be applied for time crystals, as periodically driven systems constitute counterparts of spatially periodic systems, but in the time domain. Here we show that condensed matter problems ranging from single particles in potentials of quasicrystal structure to many-body systems with exotic long-range interactions can be realized in the time domain with an appropriate periodic driving. Moreover, it is possible to create molecules where atoms are bound together due to destructive interference if the atomic scattering length is modulated in time.

DOI: 10.1103/PhysRevLett.120.140401

Although crystals have been known for years, time crystals sound more like science fiction than a serious scientific concept. In 2012 Frank Wilczek initiated a new research area by suggesting that periodic structures in time can be formed spontaneously by a quantum many-body system [1]. While the original Wilczek idea could not be realized because it was based on a system in the ground state [2–5], it turned out that spontaneous breaking of discrete time translation symmetry and self-reorganization of motion of a periodically driven quantum many-body system was possible [6]. This phenomenon was dubbed "discrete time crystals" [7–9] and it was already realized experimentally [10,11]; for a review see [12].

Apart from the realization of spontaneous breaking of discrete time translation symmetry, periodically driven quantum systems can also be employed to model crystalline structures in time in a similar way as external time-independent spatially periodic potentials allow one to model space crystals [13,14]. It should be stressed that driven systems with crystalline properties in time do not require external spatially periodic potentials. Crystal structures in time emerge due to periodic driving provided it is resonant with the unperturbed motion of a system. It is possible to investigate Anderson localization [15] in the time domain [14,16–18] or many-body localization caused by temporal disorder [19]. In the following we show that proper manipulation of higher temporal harmonics of a periodic perturbation is a perfect tool to engineer a wide class of condensed matter systems in the time domain including many-body systems with exotic interactions. Moreover, it is possible to create molecules where atoms are bound together via disordered potentials.

Let us begin with a classical single particle system in one dimension described by the Hamiltonian $H_0(x,p)$. If the motion of a particle is bounded it is convenient to perform a canonical transformation to the so-called action-angle variables [20]. Then, $H_0 = H_0(I)$ where the momentum (action) I is a constant of motion and the canonically conjugate angle θ changes linearly with time, i.e., $\theta(t) = \Omega t + \theta(0)$ where $\Omega(I) = (dH_0(I)/dI)$ is a frequency of periodic evolution of a particle. Assume we turn on a periodic driving of the form $H_1 = \lambda h(x) f(t)$ where $f(t + 2\pi/\omega) = f(t) = \sum_k f_k e^{ik\omega t}$ and λ determines the strength of the driving. The spatial part of H_1 can be expanded in a Fourier series $h(x) = \sum_n h_n(I) e^{in\theta}$. A particle is resonantly driven if the period of its unperturbed motion is equal to an integer multiple of the driving period, i.e., $\omega = s\Omega(I_0)$ where s is an integer number and I_0 is a resonant value of the action. In order to analyze motion of a particle in the vicinity of a resonant trajectory; i.e., for $I \approx I_0$, it is convenient to switch to the moving frame, $\Theta = \theta - (\omega/s)t$, and apply the secular approximation [20]. It results in the effective time-independent Hamiltonian, $H_{\rm eff} = (P^2/2m_{\rm eff}) + \lambda V_{\rm eff}(\Theta)$, where $P = I - I_0$, the effective mass $(1/m_{\rm eff}) = (d^2H_0(I_0)/dI_0^2)$ and the potential $V_{\rm eff}(\Theta) = \sum_n h_{ns}(I_0) f_{-n} e^{ins\Theta}$. If the second order corrections are negligible, which can be easily monitored [20,21], $H_{\rm eff}$ provides an exact

description of particle motion in the vicinity of a resonant trajectory.

The effective Hamiltonian, $H_{\rm eff}$, indicates that a resonantly driven system behaves like a particle on a ring, i.e., $0 < \Theta \leq 2\pi$, with a certain effective mass and in the presence of a time-independent effective potential $V_{\rm eff}(\Theta)$. If there are many nonzero Fourier components of $h(x)$, a proper choice of temporal Fourier components of $f(t)$ allows one to create a practically arbitrary effective potential. Indeed, any potential on a ring can be expanded in a series $V_{\rm eff}(\Theta) = \sum_n d_n e^{in\Theta}$ and in order to realize it we can choose the fundamental $1:1$ resonance ($s = 1$) and periodic driving with the Fourier components $f_{-n} = (d_n/h_n(I_0))$. If $s > 1$, a potential energy structure is duplicated s times. For $s \gg 1$, $V_{\rm eff}(\Theta)$ allows one to reproduce condensed matter problems where a particle can move in a potential with s identical wells of arbitrary shape and with periodic boundary conditions.

Before we illustrate our idea with an example we have to address two issues. First, so far our approach was classical but we deal with quantum systems. In order to obtain a quantum description one can either perform quantization of the effective Hamiltonian, i.e., $(P, \Theta) \to (\hat{P}, \hat{\Theta})$, or apply a quantum version of the secular approximation from the very beginning [22]. Both approaches lead to the same results. Eigenstates of the effective Hamiltonian in the moving frame correspond to time-periodic Floquet eigenstates of the original Floquet Hamiltonian, $H_F = H_0 + H_1 - i\hbar\partial_t$, in the laboratory frame [21,23]. The second issue is the following: What is the relation of the class of problems we consider with time crystals? Space crystals are related to periodic arrangement of particles in space. If we take a snapshot of a space crystal at some moment in time ($t = \text{const}$), then we can observe a crystalline structure in space. Switching to time crystals the role of time and space is exchanged. We fix position in configuration space ($x = \text{const}$); i.e., we choose the location for the detector, and ask if the probability of clicking of a detector behaves periodically in time. We have shown that in the frame moving along a classical resonant orbit, $\Theta = \theta - (\omega t/s)$, we obtain an effective Hamiltonian that can describe a solid state problem. Such a crystalline structure in Θ is reproduced in the time domain if we return to the laboratory frame, as the relation between Θ and t is linear. Thus, if we locate a detector close to a classical resonant trajectory, the probability of detection of a particle as a function of time reproduces crystalline structure described by means of $H_{\rm eff}$ in the moving frame.

In Refs. [24,25] it was proven that stable orbits of classical dissipative systems can reveal quasicrystal tiling in time. We show that quantum properties of quasicrystals in time can be investigated; see also [26,27]. In condensed matter physics quasicrystals are systems that do not have any minimal part that appears periodically in space. Nevertheless, two or more unit cells are not placed randomly because a d-dimensional quasicrystal can be constructed as a slice through a $(2d)$-dimensional periodic crystal [28–30]. We focus on the $d = 1$ case when one-dimensional quasicrystal structure can be constructed as a cut through a two-dimensional square lattice. The cut with the line whose gradient is the golden ratio generates the Fibonacci quasicrystal that can also be constructed with the help of the so-called inflation rule [24]: $B \to BS$ and $S \to B$ where B and S denote, e.g., big and small wells, respectively, of a potential energy of a single particle. Successive application of the inflation rule shows the process of growing of the quasicrystal, i.e., $B \to BS \to BSB \to BSBBS \to BSBBSBSB \to \ldots$.

In order to illustrate how to realize the Fibonacci quasicrystal in the time domain experimentally, let us consider, e.g., a particle that bounces on a vibrating mirror in the presence of a gravitational field [23,31–33] in a one-dimensional model. In the coordinate frame vibrating with the mirror, the mirror is fixed but the gravitation strength oscillates in time. Then the Hamiltonian of the system, in gravitational units [23], reads $H = (p^2/2) + x + \lambda x f(t)$ where $f(t) = \sum_k f_k e^{ik\omega t}$ and (λ/ω^2) is related to the amplitude of the mirror vibration. The secular approximation leads to the previously derived effective Hamiltonian with $m_{\rm eff} = -(\pi^2/\omega^4)$ and $h_n = -(-1)^n/(n^2\omega^2)$ if the $1:1$ resonance condition ($s = 1$) is fulfilled. A proper choice of $f(t)$ allows one to realize the effective potential $V_{\rm eff}(\Theta)$ that reproduces any finite Fibonacci quasicrystal. In Fig. 1 we show what kind of driving leads to a quasicrystal with the total number of big and small potential wells given by the seventh Fibonacci number. Transport properties in the quasicrystal that can be analyzed with the help of the effective Hamiltonian in the frame moving along the $1:1$ resonant orbit are observed in the time domain in the laboratory frame.

Now we demonstrate that periodically driven many-body systems allow for realization of solid state problems with exotic interactions. Let us illustrate this idea with ultracold atoms bouncing on a mirror that oscillates harmonically

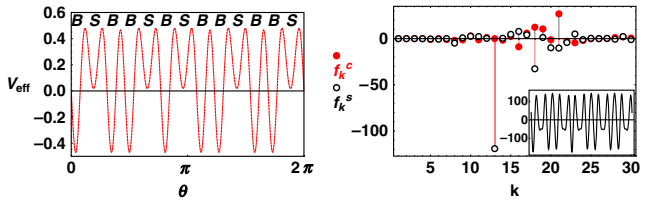

FIG. 1. Time quasicrystal: a particle bouncing on a vibrating mirror in a gravitational field in a one-dimensional model. The $1:1$ resonance condition is assumed. Left: the effective potential $V_{\rm eff}(\Theta)$ with the quasicrystal structure corresponding to the seventh Fibonacci number. Right: Fourier components of the periodic vibration of the mirror, $(f(t)/\omega^2) = \sum_k (f_k^c \cos k\omega t + f_k^s \sin k\omega t)$, that result in $V_{\rm eff}(\Theta)$ presented in the left panel. Full symbols are related to f_k^c, open symbols to f_k^s. The inset of this panel shows $(f(t)/\omega^2)$ over one period.

with frequency ω. If the s:1 resonance condition is fulfilled, the single-particle effective Hamiltonian in the moving frame reads $H_{\mathrm{eff}} = (P^2/2m_{\mathrm{eff}}) + V_0\cos(s\Theta)$ where $m_{\mathrm{eff}} = -(\pi^2 s^4/\omega^4)$ and $V_0 = -(\lambda(-1)^s/\omega^2)$. Let us assume $s \gg 1$ and V_0 sufficiently big so that in the quantum description eigenvalues of H_{eff} form well-separated energy bands and eigenstates are Bloch waves $e^{ik\Theta}v_k(\Theta)$ where $v_k(\Theta + (2\pi/s)) = v_k(\Theta)$. Note that for a fixed position in the laboratory frame, $\theta = \mathrm{const}$, the periodic Bloch waves character emerges in time, $e^{ik(\theta-\omega t/s)}v_k(\theta - (\omega t/s))$, with the period $(2\pi/\omega)$. Because of the negative effective mass m_{eff}, the effective Hamiltonian H_{eff} is bounded from above, not from below. Therefore, the first energy band possesses the highest energy. For simplicity, let us restrict ourselves to the first band and choose as the basis in the corresponding Hilbert subspace the Wannier states $w_j = w(\Theta - j(2\pi/s))$ where j denotes at which site of the effective potential a Wannier function is localized [34]. In the laboratory frame the Wannier states $w_j(x,t)$ describe localized wave packets moving along the resonant trajectory. We assume the normalization $\int_0^{s2\pi/\omega} dt\langle w_j|w_j\rangle = 1$. Thus, s sites of the effective potential in the moving frame correspond to s Wannier wave packets evolving in the laboratory frame. The width of the first energy band of H_{eff} is determined by $J = -2\int_0^{s2\pi/\omega} dt\langle w_{i+1}|H_{\mathrm{eff}}|w_i\rangle$, which is an amplitude of nearest neighbor tunnelings.

In ultracold atomic gases interactions are described by the contact Dirac-delta potential, $g_0\delta(x)$, where g_0 is determined by the atomic scattering length, which can be modulated in time by means of a Feshbach resonance [35]. We are going to show that these contact interactions between atoms can result in exotic long-range interactions in the effective description of the resonantly driven many-body system (effective long-range interactions in the phase space crystals [13,36] have been considered in [37,38]; see also [39]). For example in the case of bosonic particles, when we restrict ourselves to the Hilbert subspace spanned by Fock states $|\ldots, n_j, \ldots\rangle$, where n_j is the number of atoms occupying a mode w_j, we obtain a many-body effective Hamiltonian of the Bose-Hubbard form,

$$\hat{H}_{\mathrm{eff}} = -\frac{J}{2}\sum_{\langle i,j\rangle}\hat{a}_i^\dagger\hat{a}_j + \frac{1}{2}\sum_{i,j}U_{ij}\hat{a}_i^\dagger\hat{a}_j^\dagger\hat{a}_j\hat{a}_i, \qquad (1)$$

where the bosonic operators $\hat{a}_j$ annihilate particles in modes w_j's and $U_{ij} = \int_0^{s2\pi/\omega} dt g_0(t)u_{ij}(t)$ with $u_{ij}(t) = 2\int_0^\infty dx|w_i|^2|w_j|^2$ for $i \neq j$ and $u_{ii} = \int_0^\infty dx|w_i|^4$ [14], where we assume that the atomic scattering length $g_0(t)$ can be modulated in time. The Hamiltonian (1) is valid provided the interaction energy per particle is always smaller than the energy gap between the lowest and first excited energy bands of the single-particle system. A given interaction coefficient U_{ij} is determined mostly by $g_0(t)$ at the moment when the corresponding wave packets overlap.

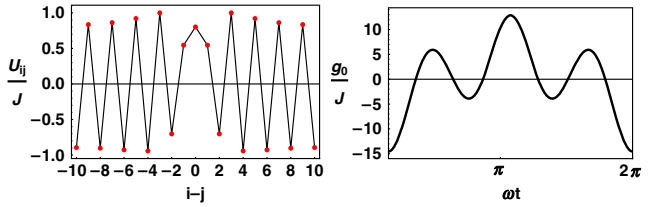

FIG. 2. System with exotic interactions: ultracold atoms bouncing on a harmonically oscillating mirror in a one-dimensional model. The 20:1 resonance condition is fulfilled and the many-body system is described by the Hamiltonian (1). The left panel shows the interaction coefficients U_{ij} corresponding to the scattering length $g_0(t)$ that is presented in the right panel. The frequency $\omega = 2.8$ of the mirror oscillations and $\lambda = 0.1$ which result in $J = 3.7\times10^{-5}$ and the gap of $302J$ between the lowest and first excited energy bands. Temporary interaction coefficients $(s2\pi/\omega)|g_0(t)|u_{ij}(t) \leq 85J$.

Suitable modulation of the scattering length $g_0(t)$ allows us to shape the interactions in (1). In order to perform a systematic analysis one can apply the singular value decomposition of the matrix $u_{ij}(t)$ where (i,j) and t are treated as indices of rows and columns, respectively. Left singular vectors tell us which sets of interaction coefficients U_{ij} can be realized, while the corresponding right singular vectors give the recipes for $g_0(t)$. In Fig. 2 we present an example of the interaction coefficients and the corresponding function $g_0(t)$. In this example the magnitude of the interactions of a particle located at a given site with other particles located at the same or distant sites is nearly the same, but their repulsive or attractive character changes in an oscillatory way.

Time is a single degree of freedom and it is hard to imagine multidimensional time crystals. However, we are going to show that resonantly driven systems can reveal properties of two-dimensional or three-dimensional space crystals in the time domain. Let us begin with a single particle bouncing between two mirrors that oscillate harmonically in two orthogonal directions with frequency ω; see Fig. 3—generalization to the three-dimensional case is straightforward. The single-particle Hamiltonian reads $H = [(p_x^2 + p_y^2)/2] + x + y + \lambda x\cos\omega t + \lambda y\cos(\omega t + \varphi)$ where φ is the relative phase of the mirror oscillations. Assuming that for each of the two independent degrees of freedom the s:1 resonance condition is fulfilled we obtain (in terms of the action-angle variables and in the moving frame $\Theta_{j=x,y} = \theta_j - (\omega t/s)$) the effective Hamiltonian, $H_{\mathrm{eff}} = [(P_x^2 + P_y^2)/2m_{\mathrm{eff}}] + V_0[\cos(s\Theta_x) + \cos(s\Theta_y)]$, which describes a particle in a two-dimensional square lattice. For $s \gg 1$, eigenstates of H_{eff} are Bloch waves $e^{i(k_x\Theta_x + k_y\Theta_y)}v_{k_x}(\Theta_x)v_{k_y}(\Theta_y)$. When we fix a position in the laboratory frame, i.e., we fix θ_x and θ_y, periodic character of Bloch waves emerges in time, $e^{i[k_x\theta_x + k_y\theta_y - (k_x+k_y)\omega t/s]}v_{k_x}(\theta_x - (\omega t/s))v_{k_y}(\theta_y - (\omega t/s))$. Different fixed values of θ_x and θ_y allow us to observe in

the time domain different cuts of the square lattice described by $H_{\rm eff}$. We restrict ourselves to the first energy band of $H_{\rm eff}$ and define the Wannier state basis $W_{\mathbf{j}} = w_x(\Theta_x - j_x(2\pi/s))w_y(\Theta_y - j_y(2\pi/s))$ where $\mathbf{j} = (j_x, j_y)$ denotes at which site of the effective potential a Wannier function is localized. In the laboratory frame the Wannier states $W_{\mathbf{j}}(x, y, t)$ describe localized wave packets moving along resonant trajectories. The shape of the trajectories depends on the relative phase φ of the mirror oscillations. For $\varphi \neq (\pi/2)$ there are s different trajectories in the configuration space and s wave packets $W_{\mathbf{j}}(x, y, t)$ moving along each of them; see Fig. 3. Thus, s^2 sites of the effective potential in the moving frame correspond to s^2 Wannier wave packets evolving in the laboratory frame. Switching to the many-body case we obtain, for ultracold bosons, a two-dimensional version of the Hamiltonian (1). If the scattering length is not modulated in time, i.e., $g_0(t) = \text{const}$, the on-site interactions are dominant and the system reproduces, in the moving frame, a two-dimensional squared lattice problem with on-site interactions [34]. If we locate detectors at different positions in the laboratory frame, the time dependence of the probabilities of detection reflects cuts of the two-dimensional square lattice; see Fig. 3.

Finally, let us show that periodic driving allows one to create a molecule where Anderson localization is responsible for the binding of two atoms. Assume that two atoms move on a ring and their scattering length is modulated in time employing a Feshbach resonance so that the Hamiltonian of the system reads $H = [(p_1^2 + p_2^2)/2] + 2\pi\lambda\delta(\theta_1 - \theta_2)f(t)$ where λ is a constant, $f(t) = \sum_{k\neq 0} f_k e^{ik\omega t}$, and $\theta_{1,2}$ denote positions of the atoms on the ring (see Fig. 4). If the first atom is moving in the clockwise direction with momentum $p_1 \approx \omega$, and the other in the anticlockwise direction with $p_2 \approx -\omega$, then the secular approximation results in $H_{\rm eff} = [(P_1^2 + P_2^2)/2] + \lambda V_{\rm eff}(\Theta_1 - \Theta_2)$ in the moving frame, i.e., $\Theta_1 = \theta_1 - \omega t$ and $\Theta_2 = \theta_2 + \omega t$. Interactions between atoms are described by the effective potential $V_{\rm eff} = \sum_n f_{-2n} e^{in(\Theta_1 - \Theta_2)}$ whose shape can be engineered at will by a suitable choice of the Fourier components f_k of the periodic driving. For example if $f_k = (1/\sqrt{k_0})e^{i\varphi_k}$ for $|k| \leq (k_0/2)$ and 0 otherwise, where $\varphi_k = -\varphi_{-k}$ are random variables chosen from a uniform distribution, the atoms interact via the effective disordered potential characterized by the correlation length $(\sqrt{2}/k_0)$ and the standard deviation λ. Then, eigenstates $\psi(\Theta_1 - \Theta_2)$ of $H_{\rm eff}$ are Anderson localized around different values θ_0 of the relative coordinate [15], i.e., $|\psi|^2 \propto e^{-|\Theta_1 - \Theta_2 - \theta_0|/l_0}$, provided the localization length $l_0 \ll 2\pi$: within the Born approximation $l_0 = (Ek_0^2/\pi\lambda^2)$, which is valid when $(\lambda^2/k_0^2) \ll E \ll (k_0^2/4)$, where E is energy of the system in the moving frame [17,40]. Hence, we are dealing with a situation where two atoms are bound together not by attractive interactions but due to destructive interference, i.e., due to the Anderson localization phenomenon induced by disordered mutual interactions [21]. If atoms are identical bosons (fermions), an eigenstate must be symmetric (antisymmetric) under their exchange. This symmetry is easily restored because we can exchange the role of the atoms. That is, the first atom can move in the anticlockwise direction, $p_1 \approx -\omega$, while the other one can

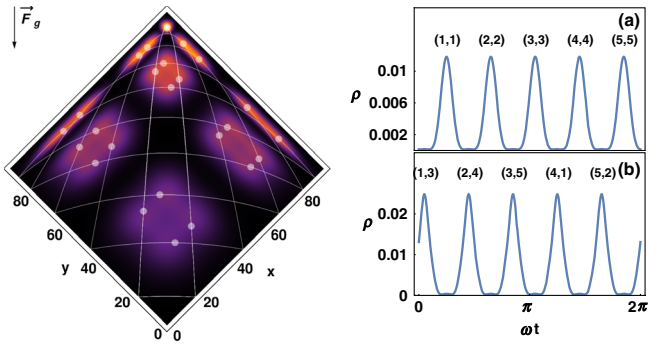

FIG. 3. Time crystal with properties of a two-dimensional space crystal: ultracold atoms bouncing between two perpendicular and harmonically oscillating mirrors with $\omega = 1.05$, $\lambda = 0.02$, and $\varphi = (\pi/2)$. The 5:1 resonance conditions are fulfilled and the many-body system is described by a two-dimensional version of the Bose-Hubbard Hamiltonian (1). For $g_0(t) = \text{const}$, the on-site interactions are dominant, i.e., $U_{ii}/g_0 \in [0.2, 0.3]J$, where different values correspond to different classical trajectories, while $U_{ij\neq i}/g_0 < 0.07J$. The left panel shows 25 Wannier wave packets, i.e., $\rho(x, y, t) = \sum_{\mathbf{j}} |W_{\mathbf{j}}(x, y, t)|^2$, at $t = (4/\omega)$ and trajectories along which they propagate—dots indicate positions of the centers of the wave packets. Two perpendicular mirrors are located at $x = 0$ and $y = 0$ and they form a $(\pi/4)$ angle with respect to the gravitational force $\vec{F}_g$. Right panels present $\rho(x, y, t)$ at $(x, y) = (90, 90)$ (a) and (82,82) (b) versus t: these plots reflect cuts of a square lattice described by the Bose-Hubbard model in the moving frame. Numbers in parentheses indicate which lattice sites $\mathbf{j} = (j_x, j_y)$ are located along the cuts.

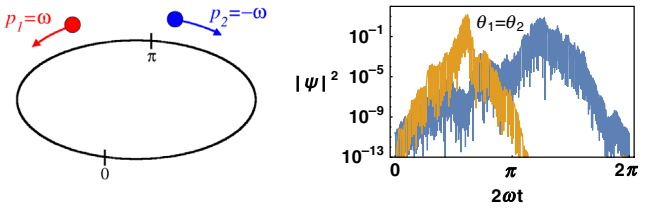

FIG. 4. Two atoms bound together due to destructive interference. The left panel shows a schematic plot of an experiment where two distinguishable atoms move on a ring in opposite directions with momenta $\pm\omega$. Resonant modulation of atomic scattering length allows one to create a molecule where the atoms are bound together due to destructive interference; i.e., in the moving frame eigenstates of the system are Anderson localized. The right panel presents probability densities for detection of the atoms at $\theta_1 = \theta_2$ in the laboratory frame versus t for two eigenstates related to energies $E = 6020$ (orange line) and 10460 (blue line) for $\lambda = 5660$ and $k_0 = 500$.

move in the clockwise direction, $p_2 \approx \omega$. Consequently, proper Floquet eigenstates for bosons or fermions, in the laboratory frame, read $\psi(\theta_1 - \theta_2 - 2\omega t) \pm \psi(\theta_2 - \theta_1 - 2\omega t)$. Experimental demonstration of two atoms bound due to destructive interference seems straightforward if atoms are prepared in a toroidal trap [41–43].

In summary, we have shown that a wide class of condensed matter problems can be realized in the time domain if single-particle or many-body systems are resonantly driven. It opens up unexplored territory for investigation of condensed matter physics in time and for the invention of novel time devices because time is our new ally. As an example we have demonstrated that periodic driving allows one to realize molecules where atoms are bound together not due to attractive mutual interactions but due to destructive interference.

Support of the National Science Centre, Poland, via Grants No. 2016/20/W/ST4/00314 (K. G.) and No. 2016/21/B/ST2/01095 (K. S.) is acknowledged. This work was performed with the support of the EU via Horizon2020 FET project QUIC (Grant No. 641122).

[1] F. Wilczek, Phys. Rev. Lett. **109**, 160401 (2012).
[2] P. Bruno, Phys. Rev. Lett. **111**, 070402 (2013).
[3] H. Watanabe and M. Oshikawa, Phys. Rev. Lett. **114**, 251603 (2015).
[4] A. Syrwid, J. Zakrzewski, and K. Sacha, Phys. Rev. Lett. **119**, 250602 (2017).
[5] F. Iemini, A. Russomanno, J. Keeling, M. Schirò, M. Dalmonte, and R. Fazio, arXiv:1708.05014.
[6] K. Sacha, Phys. Rev. A **91**, 033617 (2015).
[7] V. Khemani, A. Lazarides, R. Moessner, and S. L. Sondhi, Phys. Rev. Lett. **116**, 250401 (2016).
[8] D. V. Else, B. Bauer, and C. Nayak, Phys. Rev. Lett. **117**, 090402 (2016).
[9] N. Y. Yao, A. C. Potter, I.-D. Potirniche, and A. Vishwanath, Phys. Rev. Lett. **118**, 030401 (2017).
[10] J. Zhang, P. W. Hess, A. Kyprianidis, P. Becker, A. Lee, J. Smith, G. Pagano, I.-D. Potirniche, A. C. Potter, A. Vishwanath *et al.*, Nature (London) **543**, 217 (2017).
[11] S. Choi, J. Choi, R. Landig, G. Kucsko, H. Zhou, J. Isoya, F. Jelezko, S. Onoda, H. Sumiya, V. Khemani *et al.*, Nature (London) **543**, 221 (2017).
[12] K. Sacha and J. Zakrzewski, Rep. Prog. Phys. **81**, 016401 (2018).
[13] L. Guo, M. Marthaler, and G. Schön, Phys. Rev. Lett. **111**, 205303 (2013).
[14] K. Sacha, Sci. Rep. **5**, 10787 (2015).
[15] C. A. Müller and D. Delande, *Disorder and Interference: Localization Phenomena* (Oxford Scholarship, Oxford, 2011), Vol. 91, Chap. 9.
[16] K. Sacha and D. Delande, Phys. Rev. A **94**, 023633 (2016).
[17] K. Giergiel and K. Sacha, Phys. Rev. A **95**, 063402 (2017).
[18] D. Delande, L. Morales-Molina, and K. Sacha, Phys. Rev. Lett. **119**, 230404 (2017).
[19] M. Mierzejewski, K. Giergiel, and K. Sacha, Phys. Rev. B **96**, 140201 (2017).
[20] A. Lichtenberg and M. Lieberman, *Regular and Chaotic Dynamics*, Applied Mathematical Sciences (Springer-Verlag, Berlin, 1992).
[21] See Supplemental Material at http://link.aps.org/supplemental/10.1103/PhysRevLett.120.140401 for the analysis of the validity of effective Hamiltonians and for a short introduction to the description of periodically driven systems.
[22] G. Berman and G. Zaslavsky, Phys. Lett. **61A**, 295 (1977).
[23] A. Buchleitner, D. Delande, and J. Zakrzewski, Phys. Rep. **368**, 409 (2002).
[24] F. Flicker, arXiv:1707.09371 [SciPost (to be published)].
[25] F. Flicker, arXiv:1707.09333.
[26] T. Li, Z.-X. Gong, Z.-Q. Yin, H. T. Quan, X. Yin, P. Zhang, L.-M. Duan, and X. Zhang, Phys. Rev. Lett. **109**, 163001 (2012).
[27] Y. Huang, T. Li, and Z. Q. Yin, Phys. Rev. A **97**, 012115 (2018).
[28] J. E. S. Socolar and P. J. Steinhardt, Phys. Rev. B **34**, 617 (1986).
[29] C. Janot, *Quasicrystals: A Primer* (Oxford University Press, Oxford, 1994).
[30] M. Senechal, *Quasicrystals and Geometry* (Cambridge University Press, Cambridge, 1995).
[31] A. Steane, P. Szriftgiser, P. Desbiolles, and J. Dalibard, Phys. Rev. Lett. **74**, 4972 (1995).
[32] D. C. Lau, A. I. Sidorov, G. I. Opat, R. J. McLean, W. J. Rowlands, and P. Hannaford, Eur. Phys. J. D **5**, 193 (1999).
[33] K. Bongs, S. Burger, G. Birkl, K. Sengstock, W. Ertmer, K. Rzążewski, A. Sanpera, and M. Lewenstein, Phys. Rev. Lett. **83**, 3577 (1999).
[34] O. Dutta, M. Gajda, P. Hauke, M. Lewenstein, D.-S. Lühmann, B. A. Malomed, T. Sowiński, and J. Zakrzewski, Rep. Prog. Phys. **78**, 066001 (2015).
[35] C. Chin, R. Grimm, P. Julienne, and E. Tiesinga, Rev. Mod. Phys. **82**, 1225 (2010).
[36] L. Guo and M. Marthaler, New J. Phys. **18**, 023006 (2016).
[37] L. Guo, M. Liu, and M. Marthaler, Phys. Rev. A **93**, 053616 (2016).
[38] P. Liang, M. Marthaler, and L. Guo, New J. Phys. **20**, 023043 (2018).
[39] E. Anisimovas, G. Žlabys, B. M. Anderson, G. Juzeliūnas, and A. Eckardt, Phys. Rev. B **91**, 245135 (2015).
[40] R. C. Kuhn, O. Sigwarth, C. Miniatura, D. Delande, and C. A. Müller, New J. Phys. **9**, 161 (2007).
[41] M. Clifford, J. Arlt, J. Courtial, and K. Dholakia, Opt. Commun. **156**, 300 (1998).
[42] E. M. Wright, J. Arlt, and K. Dholakia, Phys. Rev. A **63**, 013608 (2000).
[43] Z. Y. Wang, Z. Zhang, and Q. Lin, Eur. Phys. J. D **53**, 127 (2009).